International Conference of Agricultural Engineering
AgEng 2014 Zurich 6–10 July

Ref: C0309

Path Planning for a Fruit Picking Manipulator

Jörg Baur, Christoph Schütz, Julian Pfaff, Thomas Buschmann and Heinz Ulbrich, Teschnische Universität München, Institute of Applied Mechanics, Boltzmannstr. 15, 85747 Garching, Germany

{j.baur, christoph.schuetz, julianpfaff, thomas.buschmann, ulbrich}@tum.de

Abstract

In recent years, a lot of research and development has been done in the field of autonomous harvesting in agriculture. For bulk harvesting and spraying applications (e.g. grape harvesting), there already are commercially available systems. However, automation for selective harvesting (i.e., picking) of single fruits and precision spraying applications remain challenging. Contrary to common industrial automation applications, the unstructured environment of agricultural processes lead to high demands on the design of the sensory system, the machinery in general and the planning algorithms. In our contribution we will address the path planning task for a modular agricultural manipulator with redundant kinematics. We will describe two approaches for automatically generating a path in the manipulator workspace: (1) a heuristic approach with low requirements on sensor information and (2) a potential field approach. Since the environment in agriculture applications is usually compliant (e.g. leaves or branches) only major obstacles (i.e. stems and fruits) are taken into account. The obstacles are represented by primitive objects, like cylinders and spheres. Notably, all planning algorithms are suitable for real time applications. The algorithms are implemented on a robot, which was designed and manufactured during the CROPS[1] project. It is a prototype for the harvesting of sweet-peppers, apples and grapes, as well as the precision spraying of grapes. The suitability of the algorithms will be demonstrated in a lab environment and recommendations from experiments of first field test will be discussed. As a further result, the paper will bring out the limitations, advantages and disadvantages of the proposed approaches.

Keywords: automation, harvesting robot, path planning, redundant manipulator

1 Introduction

Recently, a lot of effort was put into the automation of agricultural tasks. On the one hand, this general trend is of course driven by the farmer, to make the production more efficient. According to [Navarrete and Jeannequin2000] labor cost already makes about one third of the overall production costs for tomatoes. On the other hand, agricultural tasks may harm the workers, since they can be exposed to pesticides, rough climate or humid greenhouse conditions. Especially for bulk harvesting (e.g. grapes) there already exists a lot of commercially available machinery [Pari and Pezzi2009].

For picking of single fruits there are usually high requirements on all system components, ranging from the sensor system and detection to the manipulator and motion planning as well as the end effector design. Due to these facts there are almost no reliable or even commer-

[1] CROPS: Intelligent sensing and manipulation for sustainable production and harvesting of high-value crops - clever robots for crops (EU-project, www.crops-robots.eu).

cially available machines for selective harvesting. A notable exception is the robot for harvesting kiwi fruits developed by [Scarfe et al.2009] in a research project.
In the CROPS project we aim (amongst other things) at the development of a modular robot and its algorithms, suitable for several agricultural applications. In Figure 1 typical cultivation scenes of the three selective harvesting applications (apples, grapes and sweet pepper) are illustrated. Another application is the precision spraying of fruits, which was already successfully accomplished in the project and published by [Oberti et al.2013]. In this publication, we will describe the path planning algorithms, which are implemented on the CROPS manipulator.

Figure 1: Harvesting applications in the CROPS project: apples (left), grapes (middle) and sweet pepper (right).

2 Requirements and Specifications

The general requirements on the manipulator work space and its kinematic design for the sweet pepper harvesting application have already been described in [Baur et al.2012] and [Schuetz et al.2014]. This application has the highest demands on the manipulator kinematics since it requires high dexterity of the arm in a very narrow work space. The cultivation of apples and grapes in the CROPS project is done in an espalier system, which is suitable for automation. Challenges for these harvesting applications are the occurrence of clusters or pairs of fruits. However, this problem will not be addressed in this publication.

3 Motion Planning

The goal of the motion planner is the generation of a joint trajectory which is feasible for the manipulator and brings the tool-center-point (TCP) from a start pose to the goal pose. Feasible in this case means that the trajectory can be tracked by the real robot and self-collisions are avoided. An approach which takes into account all obstacles was not considered, since in the workspace of the manipulator are leaves, stems and other fruits which in general cannot be avoided due to the dimensions of the end-effector and the manipulator itself. The path planning scheme is hierarchically organized in two main levels: The first level is the generation of a parameterized trajectory $\boldsymbol{w}_d(t)$ in the manipulator workspace. This could, for example, be a straight line path, which is the simplest and also the most natural path for human beings to grasp objects. On the second level, the work space trajectory is fed to an inverse kinematics algorithm to obtain the joint trajectory $\boldsymbol{q}_d(t)$ for the low level joint controllers (if the motion is feasible). The scheme is illustrated in Figure 2. All algorithms, the workspace planning and the inverse kinematics are suitable for real time application. In Section 3.1 two different approaches for work space planning are introduced, while Section 3.2 briefly deals with the inverse kinematics computation.

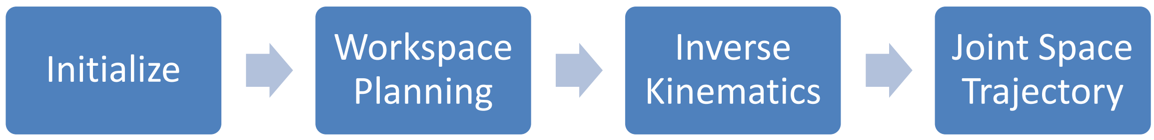

Figure 2: General overview of the path planning scheme.

3.1 Workspace Planning

3.1.1 Heuristic Approach for Harvesting

By exploiting known facts of the environment, a heuristic algorithm for trajectory generation has been designed. Although this approach does not provide a general solution, it will lead to successful results in many practical scenarios in our laboratory. Furthermore, this method has minimal demands regarding knowledge on the environment and thus it poses low requirements on the sensor system. The heuristic algorithm will be explained for the sweet pepper application but can be applied to the other scenarios with few modifications.
When approaching the fruit, a collision of the manipulator with the main stem must be avoided while the target must be approachable. With a gripping end-effector, a radial approach, i.e. fruit center in line with the stem center, seems the most promising in avoiding collisions. Initially, the planning algorithm reduces the task into a two dimensional problem. Figure 3 shows the top view of the planning scene with the start position $\boldsymbol{r}_s$, the fruit center position $\boldsymbol{r}_g$and the stem center position $\boldsymbol{r}_{st}$ in (x, y) – Cartesian coordinates. Besides moving the end-effector from the start to the goal position, the desired properties of the workspace planner are the following:

- Input for the planner: TCP start position, stem center coordinates and the fruit center coordinates.
- A circular area around the stem with radius r_e must be avoided until the entry point $\boldsymbol{r}_e$ is reached. At the entry point, the goal orientation should be obtained and the end-effector must move in a straight line from $\boldsymbol{r}_e$ to $\boldsymbol{r}_g$.
- Output of the planner: The desired trajectory $\boldsymbol{w}_d(t)$ with zero velocity at the beginning and at the end.

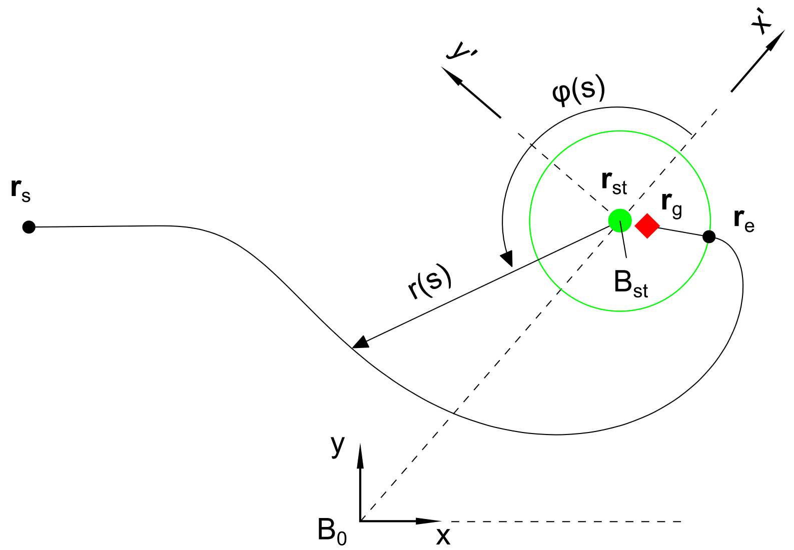

Figure 3: Top view of the planar planning scene. The fruit is indicated in red, the stem center in dark green and the plant area in green.

A description of the path in the polar coordinates

$$\phi = (r(s), \quad \varphi(s))^T \tag{3-1}$$

with respect to the stem frame B_{st} (origin at the stem center) seems natural. The scalar function $s(t) \in [0,1]$ is a path parameter for time parameterization.

The Cartesian coordinates $\boldsymbol{r}_s$ and $\boldsymbol{r}_g$ are easily transformed into the corresponding polar coordinates $\boldsymbol{\phi}_s = (r_s, \varphi_s)^T$ and $\boldsymbol{\phi}_g = (r_g, \varphi_g)^T$. The polar coordinates of the entry points are given by $\boldsymbol{\phi}_e = (r_e, \varphi_g)^T$, with the entry radius parameter r_e. According to the requirements, the following constraints hold:

$$\boldsymbol{\phi}(s = 0) = \boldsymbol{\phi}_s \tag{3-2}$$
$$\boldsymbol{\phi}(s = s_e) = \boldsymbol{\phi}_e \tag{3-3}$$
$$\boldsymbol{\phi}(s = 1) = \boldsymbol{\phi}_g \tag{3-4}$$

Here, $0 < s_e < 1$ denotes the parameter when the entry point must be reached. The constraints (3-2)-(3-4) can be fulfilled with the following piecewise defined curves:

$$r(s) = \begin{cases} e^{-a\,s} + b & 0 \le s \le s_e \\ \bar{r} = \sum_{i=0}^{5} r_i s^i & s_e < s \le 1 \end{cases} \tag{3-5}$$

$$\varphi(s) = \begin{cases} \varphi_s & 0 \le s \le s_a \\ \bar{\varphi} = \sum_{i=0}^{5} \varphi_i s^i & s_a < s \le s_e \\ \varphi_g & s_e < s \le 1 \end{cases} \tag{3-6}$$

And the parameter a and b are obtained as:

$$a = \frac{1}{s_e \ 1/(r_e - b)} \qquad \text{and} \qquad b = r_s - 1 \tag{3-7}$$

The coefficients for the fifth order polynomials $\bar{r}$ and $\bar{\varphi}$ can be calculated with the appropriate boundary and transition conditions. Figure 4 shows the paths calculated with the planner.

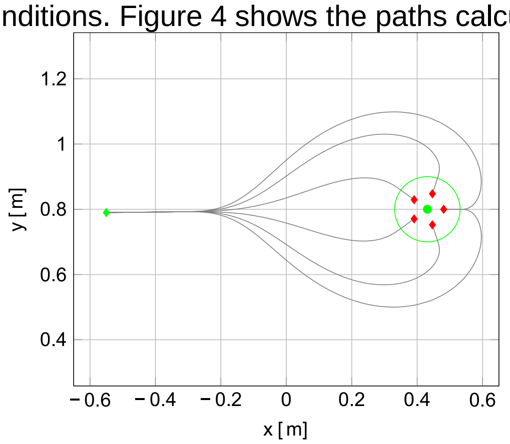

Figure 4: Resulting paths in the plane with the heuristic planner for several goals ($r_e = 0.1m$, $s_e = 0.1$ and $s_a = 0.8$). The goals are indicated by red diamonds, the stem by a green dot and the entry zone with a green circle.

3.1.2 Potential Field Method

A common approach in motion planning is the application of artificial potential function. Basically, it is the combination of an attractive (goal) and repulsive (obstacles) potential functions

[Siciliano et al.2009]. To avoid the occurrence of local minima, we will apply so called navigation functions with the property of a unique minima. Additionally, only spherical obstacles will be considered. According to [Choset et al.2005] the navigation potential function ϕ is given by:

$$\phi(\boldsymbol{x}) = \frac{d(\boldsymbol{x},\boldsymbol{x}_g)^2}{\left[d(\boldsymbol{x},\boldsymbol{x}_g)^{2\kappa} + \beta(\boldsymbol{x})\right]^{1/\kappa}} \tag{3-8}$$

Here $\boldsymbol{x}_g \in \mathbb{R}^n$ is the target, $d(\boldsymbol{x},\boldsymbol{x}_g)$ the Euclidean distance between two vectors ($\boldsymbol{x} \in \mathbb{R}^n$ and $\boldsymbol{x}_g$), κ is a parameter and β is the product of the attractive potential of the bounding sphere with radius r_0, centered at $\boldsymbol{x}_0$ and the repulsive function of the N sphere obstacles with center at $\boldsymbol{x}_i$ and radius r_i:

$$\begin{aligned} \beta &= \prod_{i=0}^{N} \beta_i(\boldsymbol{x}) \\ \beta_0 &= -d(\boldsymbol{x},\boldsymbol{x}_0)^2 + r_0{}^2 \\ \beta_i &= d(\boldsymbol{x},\boldsymbol{x}_i)^2 - r_i{}^2 \end{aligned} \tag{3-9}$$

Applying the algorithm of steepest descent, starting at any point within the bounding sphere $\boldsymbol{x}_s$ (with the gradient of (3-8)), the minimum of the potential function can be found while the iterations of the optimization describe the path. Exemplary, in Figure 5 the algorithm was applied to a two dimensional scene ($n = 2$) with three obstacles ($N = 3$). The potential function is plotted on the left hand side. At the target, the value of the potential function is $\phi = 0$ while at the obstacles and beyond the bounding sphere it approaches $\phi = 1$. On the right hand side of Figure 5 the corresponding contour plot is shown. One can clearly see the obstacles (indicated by green circles) as well as the start (green diamond) and target position (red diamond). The path obtained by the gradient method is illustrated in black.

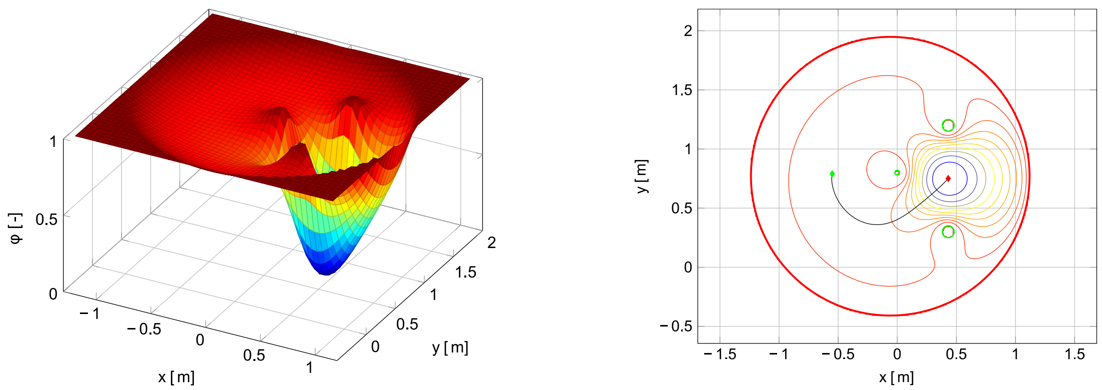

Figure 5: Potential field (left) and contour plot (right) with spherical obstacles (green circles) and path (black) from start to goal by minimizing the potential with steepest descent.

The potential field method was applied to the same world scene as the heuristic planner (cf. Figure 4). The resulting paths are shown in Figure 6. Note that each path is computed with only one (stem) spherical obstacle and the results are illustrated in one plot.

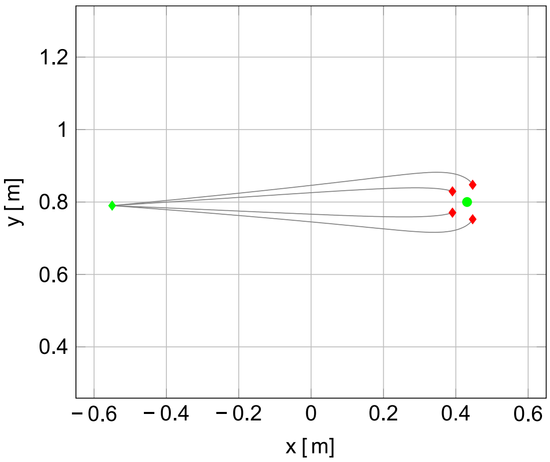

Figure 6: Resulting paths in the plane with the navigation potential function planner for several goals (red diamonds) and one stem obstacles (green sphere).

3.2 Inverse Kinematics

With the planner described above the desired work space trajectory $\boldsymbol{w}_d, \dot{\boldsymbol{w}}_d$ is obtained. The corresponding joint trajectories $\boldsymbol{q}, \dot{\boldsymbol{q}}$ are obtained with an inverse kinematics algorithm. We apply the following equation, suitable for redundant manipulators [Liégeois1977], [Nakamura1990]:

$$\dot{\boldsymbol{q}} = \boldsymbol{J}^{\#}\dot{\boldsymbol{w}}_d - k\left(\boldsymbol{I} - \boldsymbol{J}^{\#}\boldsymbol{J}\right)\left(\frac{\partial H}{\partial \boldsymbol{q}}\right)^T \tag{3-10}$$

Here, the Jacobian matrix and its pseudo-inverse is denoted by $\boldsymbol{J}$ and $\boldsymbol{J}^{\#}$, the scalar parameter k is a gain and $H(\boldsymbol{q})$ is a cost functional which can be used for secondary objectives like joint limit and self-collision avoidance. The joint positions are obtained by numerical integration of (3-10). More details on the algorithm for our application were already reported in [Baur et al.2012], [Baur et al.2013], [Schwienbacher et al.2011] and will not be discussed here.

4 Results and Discussion

An evaluation of the planning algorithms has been performed with the first manipulator prototype developed at our lab and the first end-effector prototype developed by *FESTO* [Gauchel and Saller2012]. To compare both algorithms, the same scene was investigated. According to Sect. 3.1.1, the scene can be described by the target position $\boldsymbol{r}_g \in \mathbb{R}^3$ (e.g. fruit center position) and the stem center position $\boldsymbol{r}_{st} \in \mathbb{R}^2$. With this input, the path is planned from the start to the target position. For our application, the workspace fully defines the TCP pose in the three dimensional space. This can be parameterized by Cartesian coordinates and Cardan angles: $\boldsymbol{w} = (x, y, z, \alpha, \beta, \gamma)^T$. To fully describe the work space, the path of the planners (given in the (x, y)-plane) are completed by an interpolation of z (from start to goal), and of α and β (from start to $\alpha = \beta = 0$). The goal orientation γ is defined by the tangent of the path (in the (x, y)-plane) at the goal position and is then correspondingly interpolated. The resulting paths and the manipulator configurations, calculated by the inverse kinematics algorithm (cf. Sect. 3.2) are shown in Figure 7 and Figure 8. In Figure 7 a fruit, located “in front” of the stem was approached, while in Figure 8 the fruit is “behind” the stem. On the one hand, the results indicate that with the heuristic planning, the plant area is avoided until the fruit is grasped. However, according to Figure 8 (right) this is not true for the potential field approach. On the other hand, with the heuristic planning, the manipulator sweeps through a rather large area in the work space, compared to the planning with the potential field approach. This will increase the risk in collisions with the manipulator and other plants or fruits. In addition, due to the goal pose resulting with the heuristic planning (see Figure 8, left) the number of reachable fruits decrease due to the kinematics, when the plant (stem and fruit) move further to the right.

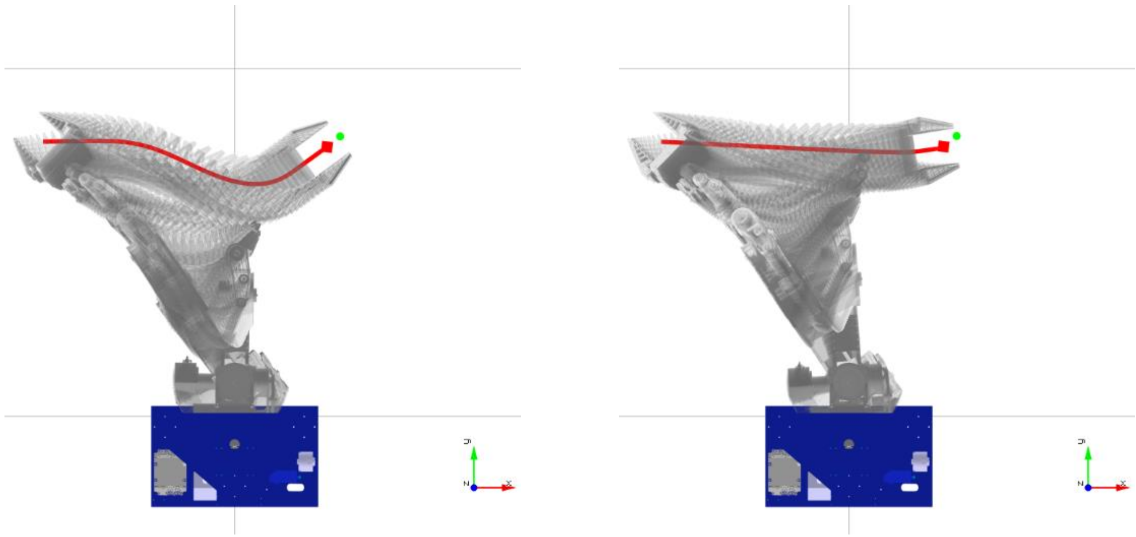

Figure 7: Resulting robot configurations (gray) and TCP path (red) for the heuristic planning (left) and potential navigation function (right). The stem is indicated by a green dot and the fruit center with the red diamond.

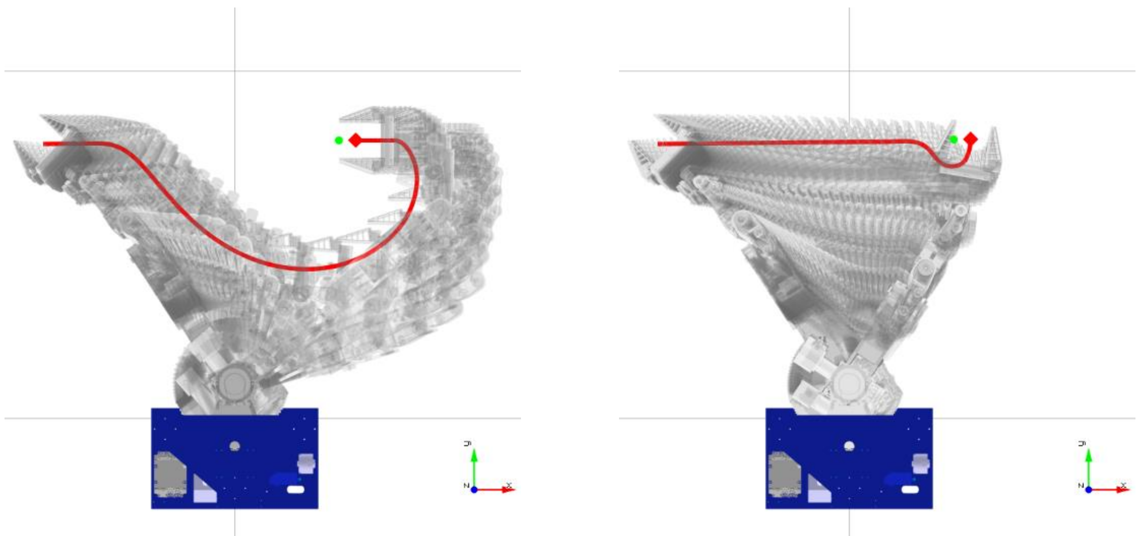

Figure 8: Resulting robot configurations (gray) and TCP path (red) for the heuristic planning (left) and potential navigation function (right). The stem is indicated by a green dot and the fruit center with the red diamond.

Although the planning with the potential field approach can deal with more general cases, we choose the heuristic planning for the implementation in our laboratory demonstration [Schuetz et al.2014], since it is ensured, that the gripper approaches the fruit without colliding with the stem. The results are promising and many fruits were harvested. Experiments in greenhouses showed, however, that accurately detecting the stem belonging to the fruit that is to be harvested is not straightforward.

5 Conclusion

In this publication we gave a general overview on the planning algorithm for the harvesting manipulator in the CROPS project. Two different approaches to plan a work space trajectory, namely a heuristic and a potential field method were described. The results of the planner in a world scene with one fruit and one stem (corresponding to the sweet pepper application) were shown and discussed. For a single free standing plant, the heuristic planner was successfully tested in our laboratory demonstration.

6 Acknowledgment

This research is co-funded by the European Union (CROPS GA no 246252). Special thanks go to G. Mayr, S. Gerer, and G. König for their technical support and contributions to the electrical and mechanical design. The authors would also like to thank the project partners in the CROPS consortium for their assistance and input during the derivation of the manipulator requirements and the field experiments.

7 References

[Baur et al.2013] Baur, J., Pfaff, J., Schuetz, C., and Ulbrich, H. (2013). Dynamic modeling and realization of an agricultural manipulator. In *Proceedings of XV International Symposium on Dynamic Problems of Mechanics, DINAME*.

[Baur et al.2012] Baur, J., Pfaff, J., Ulbrich, H., and Villgrattner, T. (2012). Design and development of a redundant modular multipurpose agricultural manipulator. In *Advanced Intelligent Mechatronics (AIM), 2012 IEEE/ASME International Conference on*, pages 823–830, Kaohsiung, Taiwan.

[Choset et al.2005] Choset, H., Lynch, K. M., Hutchinson, S., Kantor, G. A., Burgard, W., Kavraki, L. E., and Thrun, S. (2005). *Principles of Robot Motion: Theory, Algorithms, and Implementations*. MIT Press, Cambridge, MA.

[Gauchel and Saller2012] Gauchel, W. and Saller, S. (2012). Adaptive gripper jaws for high-value crops harvesting. In *8th International Conference on Fluid Power (8th IFK) in Dresden*.

[Liégeois1977] Liégeois, A. (1977). Automatic supervisory control of the configuration and behavior of multibody mechanisms. *IEEE Transactions on Systems, Man, and Cybernetics*, 7:868–871.

[Nakamura1990] Nakamura, Y. (1990). *Advanced Robotics: Redundancy and Optimization*. Addison-Wesley Longman Publishing Co., Inc., Boston, MA, USA, 1st edition.

[Navarrete and Jeannequin2000] Navarrete, M. and Jeannequin, B. (2000). Effect of frequency of axillary bud pruning on vegetative growth and fruit yield in greenhouse tomato crops. *Scientia Horticulturae*, 86(3):197 – 210.

[Oberti et al.2013] Oberti, R., Marchi, M., Tirelli, P., Calcante, A., Iriti, M., Hocevar, M., Baur, J., Pfaff, J., Schuetz, C., and Ulbrich, H. (2013). Šelective spraying of grapevines diseases by a modular agricultural robot. In *Journal of agricultural engineering*, volume 44, pages 149–153.

[Pari and Pezzi2009] Pari, L. and Pezzi, F. (2009). Evaluation of two grapes harvesting machine with horizontal and vertical shaking. In *CIGR Proceedings, Technology and Management to Increase the Efficiency in Sustainable Agricultural Systems*, pages 1–5, Rosario, Argentina.

[Scarfe et al.2009] Scarfe, A., Flemmer, R., Bakker, H., and Flemmer, C. (2009). Development of an autonomous kiwifruit picking robot. In *4th International Conference on Autonomous Robots and Agents, ICARA*, pages 380–384.

[Schuetz et al.2014] Schuetz, C., Pfaff, J., Baur, J., Buschmann, T., and Ulbrich, H. (2014). A modular robot system for agricultural applications. In *International Conference on Agricultural Engineering*.

[Schwienbacher et al.2011] Schwienbacher, M., Buschmann, T., Lohmeier, S., Favot, V., and Ulbrich, H. (2011). Self-collision avoidance and angular momentum compensation for a biped humanoid robot. In *Robotics and Automation (ICRA), 2011 IEEE International Conference on*, pages 581 –586.

[Siciliano et al.2009] Siciliano, B., Sciavicco, L., and Villani, L. (2009). *Robotics: modelling, planning and control*. Springer Verlag.